Shock and Vibration 17 (2010) 219–231
DOI 10.3233/SAV-2010-0507
IOS Press

Shaker random testing with low kurtosis: Review of the methods and application for sigma limiting

Alexander Steinwolf*
Department of Mechanical Engineering, University of Auckland, Auckland, New Zealand

Received 16 July 2007
Revised 2009

Abstract. The non-Gaussian random shaker testing with kurtosis control has been known as a way of increasing the excitation crest factor in order to realistically simulate ground vehicle vibrations and other situations when the time history includes extreme peaks higher than those appearing in Gaussian random signals. However, an opposite action is also useful in other applications, particularly in modal testing. If the PSD is the only test specification, more power can be extracted from the same shaker if the crest factor is decreased and an extra space is created between the peaks of reduced height and the system abort limit. To achieve this, a technique of sigma clipping is commonly used but it generates harmonic distortions reducing dynamic range of shaker system. It is shown in the paper that the non-Gaussian phase selection in the IFFT generation can reduce kurtosis to 1.7 and bring the crest factor of drive signals from 4.5 to 2. The phase selection method does this without any loss of the controller's dynamic range that inevitably occurs after sigma clipping or polynomial transformation of time histories.

1. Introduction

Shaker controllers for random vibration testing can be based on the well-established FFT/IFFT data processing technique. In so doing, a test specification is given in frequency domain in terms of power spectral density (PSD) and actual time histories are reconstructed from the prescribed PSD by the inverse Fourier transform. The latter means that the shaker is driven by a multi-frequency signal with a large number of harmonics N

$$x(t) = \sum_{n=1}^{N} A_n \cos(2\pi n \Delta f t + \varphi_n). \tag{1}$$

The amplitudes A_n of the harmonics are determined

$$A_n = \sqrt{2\Delta f S(n\Delta f)} \tag{2}$$

according to the given PSD shape $S(f)$ that is discretized with the frequency increment Δf. The phase angles φ_n are defined as samples of a random variable uniformly distributed in the range from 0 to 2π.

The excitation obtained with various sets of random phases is a pseudo-random signal with discrete spectrum. A technique of windowing and overlapping time history blocks generated according to Eq. (1) can be implemented [9, 18] to make the resulting signal closer to true-random with a continuous spectrum. The windowing also helps to remove discontinuities of the signal at the data block boundaries and avoid leakage.

*Corresponding author. E-mail: a.steinwolf@auckland.ac.nz.

ISSN 1070-9622/10/$27.50

The discrete Fourier transform model is handy for digital random controllers because it allows easy correction of the input PSD shape using the acceleration feedback signal collected from the unit under test. A closed-loop iteration procedure is arranged for this purpose as follows. The height of a certain spectrum line $S_i^{acc}(n\Delta f)$ located at the frequency $f = n\Delta f$ in the acceleration feedback PSD on i-th iteration may become more (or less) than what it should be according to the test specification $S_{spec}(n\Delta f)$ at this frequency. To compensate for the difference between $S_i^{acc}(n\Delta f)$ and $S_{spec}(n\Delta f)$, the height of the same spectrum line $S_{i+1}^{dr}(n\Delta f)$ in the drive signal PSD on the next $(i+1)$–th iteration should be decreased (or increased) compared to what it was on the previous iteration $S_i^{dr}(n\Delta f)$.

Mathematically the above can be expressed by the following equation

$$S_{i+1}^{dr}(n\Delta f) = S_i^{dr}(n\Delta f)\frac{S_{spec}(n\Delta f)}{S_i^{acc}(n\Delta f)} \quad , \qquad n = 1, 2, 3, \ldots, N. \tag{3}$$

Equation (3) being repeated for each of N spectrum lines gives the full PSD of the drive signal for the next iteration. Then all discrete spectrum values $S_{i+1}^{dr}(n\Delta f)$ obtained are substituted into Eq. (2) and a new drive signal time history is generated according to Eq. (1). Such iterations can be continued until the acceleration feedback spectrum $S_i^{acc}(n\Delta f)$ is close enough to the specified target profile $S_{spec}(n\Delta f)$.

This classic technique for simulating random excitations on shakers can be updated [14–17] to involve non-Gaussian characteristics such as kurtosis and to control them in the same closed-loop iterative manner as the PSD. If the kurtosis value K_i^{dr} of drive signal is increased, the kurtosis of the acceleration feedback K_i^{acc} will follow or vice versa if the kurtosis decrease is needed. Hence the kurtosis can be adjusted similarly to how it was discussed above for the height of a PSD line

$$K_{i+1}^{dr} = K_i^{dr}\frac{K_{spec}}{K_i^{acc}} \tag{4}$$

with only one such correction for the entire random signal, not N corrections as for the PSD.

If the windowing and overlapping procedure is applied, the kurtosis after windowing and overlapping will be closer to the Gaussian value than it was for the original pseudo-random signal (1). This issue was addressed in Reference [17] where equations were derived for calculating the change in kurtosis depending on the window type and the overlap number. These results are useful when assigning the K_1^{dr} value for the pseudo-random drive signal on the first non-Gaussian iteration. Then, the influence of windowing and overlapping will be taken into account when using Eq. (4) on the second and further iterations.

Non-Gaussian methods allowed revival of the simulation approach to random shaker testing. It has been undeservedly overshadowed in recent times by the Time Waveform Replication methodology that is, of course, excellent in reproducing a particular road sample but fails to provide a test representing this road type generally (more detail and data examples are given in Reference [15]). Thus, the in-house shaker testing for environmental excitations has already benefited from the new ability to increase kurtosis. Now, other applications may require to go the other way around and to develop procedures for kurtosis decrease.

2. Methods of simultaneous PSD and kurtosis closed-loop control

Two methods of non-Gaussian closed-loop shaker control with IFFT generation have been suggested and realized experimentally. The *method of Gaussian-to-non-Gaussian polynomial transformation* operates with instantaneous values of the original Gaussian signal. Initially, this method was recommended in the form [10,11] where non-Gaussian time histories are first prepared offline before running a test and, then, these time histories are reproduced on the shaker in the Time Waveform Replication mode. It was only later when the polynomial transform was extended and modified [14,15] into a method that can be used in the closed-loop frequency domain control mode. With such an approach, the polynomial transform becomes just a post-IFFT signal transformation addition, still in the frame of the regular closed-loop FFT/PSD shaker testing.

The polynomial transform is easy to implement but it significantly reduces the controller's dynamic range compared to the traditional Gaussian random testing. Insufficient dynamic range disrupts the PSD shape if any resonances of

the unit under test or the shaker armature are present in the excitation frequency band. It is not possible to achieve low enough PSD level for the drive signal at resonance frequency because of uncontrolled harmonic distortions introduced by the nonlinear polynomial transform (see experimental results in References [14,15]). There is no such difficulty with the *special phase selection method* [14–16] because nothing is done to the signal after the IFFT generation, i.e. small PSD values are not disturbed at all.

Since the power spectrum does not depend on the harmonics phases, they can be manipulated to accomplish non-Gaussian simulation. The essence of the phase selection method is that the variables are separated: the amplitudes are still responsible for the PSD according to Eq. (2), whereas the phases φ_n are not random all as they were in the classic IFFT generation. Instead, some of the phases are now used to adjust kurtosis. Thus, both characteristics, the PSD and the kurtosis, are controlled independently of each other. It is important that the PSD and kurtosis corrections by Eqs (3) and (4) can be done simultaneously in the same iteration process to save the controller's loop time.

Leading controller manufacturers, such as Vibration Research, Unholtz-Dickie, and IMV, have recognized the need for non-Gaussian random testing and started using it [4,6,20]. Currently, their research and development is restricted only to the kurtosis increase. The motivation for this objective was established in References [14–17, 20]. It is about a necessity to achieve a higher crest factor of the excitation time history because road transportation data typically contains occasional extreme peaks that are missing in the Gaussian random shaker simulation by the PSD/FFT approach.

Contrary to high kurtosis resulting in spiky time histories distinct from those of Gaussian random signals, an opposite action of kurtosis decrease is expected to generate a pseudo-random excitation with the time history smoother than Gaussian. This paper discusses how the latter can be achieved and whether the shaker vibration with less prominent peaks (i.e. with a lower crest factor) can still have the same PSD specification as a regular Gaussian excitation. This new kind of non-Gaussian random simulation has certain applications in the shaker testing industry.

Long before the non-Gaussian control with kurtosis increase was introduced for shaker testing in the last decade, the other direction of departing from the Gaussian random excitation "downwards" has been actually in use though not by kurtosis control but via direct crest factor modification. Reducing the crest factor by sigma clipping is a practice that shaker test engineers know about. A relevant option is available in standard FFT random controllers.

Sigma clipping is used to protect the shaker amplifier from being overloaded above its peak-handling capacity. One more purpose of clipping is to limit the peak acceleration generated by the system because displacement of the shaker drive coil should not exceed the value that was expected for the implemented design of the dc magnetic field air gap within which the drive coil is moving. However, controller manuals and websites warn that the sigma clipping technique does have its drawbacks [21].

Signal clipping produces frequency distortions because the square-wave shape of clipped peaks results in energy leaking across the test bandwidth interval and beyond it. These frequency distortions increase the PSD "noise floor" and this can significantly reduce the system's ability to control sharp resonances. As the non-Gaussian random shaker control with low kurtosis would decrease the crest factor, i.e. provide another way of sigma limiting, this could be a useful alternative to avoid the frequency distortions downside of traditional sigma clipping.

3. Kurtosis and crest factor

Implementation of non-Gaussian random simulation in shaker testing means controlling a much wider diversity of probability distributions of the generated excitations. Various deviations from the Gaussian model can be considered but this study focuses on what is the probability of occurrence of time history peaks with the height of several root-mean-square values. In other words, we look at how frequent and prominent high peaks are in a time history block of a limited length. This is described by the kurtosis parameter

$$K = \frac{M_4}{\sigma^4} = \frac{1}{\sigma^4} \int_{-\infty}^{\infty} x^4 P(x) dx \tag{5}$$

that is associated with the fourth central moment M_4 of the signal probability density function (PDF) denoted $P(x)$ in the above equation. The root-mean-square (RMS) value σ of the signal is also involved.

If the Gaussian PDF, that is $P_G(x) = \exp(-x^2/2\sigma^2)/(\sigma\sqrt{2\pi})$, is substituted into Eq. (5), the integral results in $3\sigma^4$ making the kurtosis value equal to 3, regardless of what is the RMS value σ of the signal under consideration. So, if a random signal is Gaussian then $K = 3$ is the exact theoretical value for its kurtosis. If the signal is non-Gaussian with high time history peaks being more frequent, then $P_{nG}(x) > P_G(x)$ for large arguments x. With such an increase of integrand, the result of integration in Eq. (5) becomes not $3\sigma^4$, but more, making the kurtosis $K > 3$. In the opposite case of $P_{nG}(x) < P_G(x)$, the corresponding kurtosis value is $K < 3$.

The above is a useful alternative to characterizing signal peak heights by the well-known crest factor parameter that is a ratio between the absolute maximum of the signal and its RMS value

$$CF = \frac{|x(t)|_{\max}}{\sigma}. \tag{6}$$

The kurtosis parameter (5) is more robust because, being an integral-based characteristic, it summarizes the effect of various extreme peaks. The crest factor (6) is not as comprehensive and takes into account only a single peak, the one that is the largest in the captured time history. Furthermore, in contrast to kurtosis, no strict theoretical value can be defined for the crest factor of a Gaussian signal because the magnitude of the largest peak depends on the length of a time history sample.

Hence, it is harder to quantify the non-Gaussian deviations in terms of crest factor than in terms of kurtosis. In practice, for record lengths typical in shaker testing, $CF = 4 - 4.5$ can be considered as corresponding to the Gaussian kurtosis value $K_G = 3$. It is most important that, for non-Gaussian random signals, the kurtosis and the crest factor follow the same pattern, departing from the above values either up or down but both in the same direction.

4. Applications of low kurtosis random testing

Techniques for closed-loop random testing with kurtosis increase were developed first [6,14–16,20] to raise the crest factor in order to realistically simulate ground vehicle vibrations and other situations when the time history includes excessive peaks higher than those appearing in Gaussian random signals. However, an opposite action of crest factor decrease is also useful for other, not less important, test specifications.

When using pseudo-random excitations for experimental modal analysis [1,3,5], it is not about simulating realistic time history data and high peaks specifically. A broadband excitation with a flat PSD is required to identify resonances and notches in the dynamic system response. If the prescribed PSD could be achieved not with the common Gaussian crest factor $CF > 4$ but with something substantially lower, then the advantages would be: more power delivered by the shaker, less risk of damage to the unit under test, better signal-to-noise ratio, etc. The first of these benefits is particularly attractive.

Assume that a controller drives a shaker to its power limit of producing random vibration with RMS of σ m/s^2 but a further increase of RMS is not possible because the peak value of 4σ m/s^2 is what corresponds to the amplifier/shaker peak abort limits. If the controller could operate the shaker so that the crest factor is reduced, then the same limiting peak height of 4σ m/s^2 would be possible with the RMS value not of σ m/s^2 but more, in exactly the same proportion at which the crest factor was reduced. Such an increase of the RMS value means that the power delivered by the shaker system would be greater.

For example, let the RMS be 100 m/s^2 and the crest factor – initially equal to 4 in the Gaussian random controller mode. Then, by switching to the non-Gaussian mode with kurtosis decrease and reducing crest factor to 2.5, the acceleration peak value would be changed from 400 to 250 m/s^2. This extra room created between 400 and 250 m/s^2 allows to increase the RMS up to 160 m/s^2 still having the peak value within the initial 400 m/s^2 limit because $CF = 2.5 =$ (400 m/s^2)/(160 m/s^2). The fact that the RMS value has increased from 100 to 160 m/s^2 means that the same shaker with the same abort limit delivers 2.5 times more powerful excitation now.

Apart from modal testing, low kurtosis and crest factor might be useful when there is a strong periodic component in the vibration to be simulated on shaker. This is the case in helicopters, propeller aircraft, ICE engines and other machines and vehicles with a fast heavy rotor. For example, kurtosis and crest factor for a sinusoidal signal are as low as $K = 1.5$ and $CF = 1.41$.

When a single harmonic component is combined with random background vibration, the kurtosis will rise but still remain lower than the Gaussian value of 3. Depending on how strong the sinusoidal component is in comparison

with the additive random noise, something between $K = 2$ and $K = 2.5$ can be expected. A similar tendency is inherent when not one but a few harmonics are present in the periodic component. This kind of test specification is harder to set up accurately and an ability of low kurtosis simulation could be helpful in this case.

5. Polynomial transformation decreasing kurtosis

The first idea that comes to mind about how to advance from a signal with the Gaussian probability distribution to a non-Gaussian signal is to generate a Gaussian time history and, then, to modify it with a help of functional transformation $y = f(x)$ that converts digitized instantaneous values of the initial signal (1) one by one into a new signal. The transformation can be conveniently prescribed in polynomial form with a third-order polynomial sufficient for kurtosis manipulations.

To increase kurtosis [10,11,15], let $x(t)$ be the standardized Gaussian signal (with zero mean and RMS equal to 1) and calculate the transform as

$$y(t) = \alpha_1 x(t) + \alpha_3 x^3(t). \tag{7}$$

Then, the cubic term governed by an appropriate choice of the coefficient α_3 will stretch those $x(t)$ values that are larger than 1. This action changes the distribution of instantaneous values making high peaks to leap out of the background time history further. As a result, the transformed signal $y(t)$ acquires higher kurtosis and crest factor.

To decrease kurtosis and crest factor an opposite effect is needed of the Gaussian signal having more prominent peaks than the transformed signal. Thus, the same Eq. (7) can be used [10,22] to model the required change in peak behavior but now $y(t)$ must be the standardized Gaussian signal and $x(t)$ must become the transformed signal with lower kurtosis and crest factor. Analytical solution was obtained in Reference [22] for how the coefficients α_1 and α_3 should be expressed via the desired kurtosis value K_d

$$\alpha_1 = h(1 - 3\beta), \quad \alpha_3 = h^3\beta \tag{8}$$

where $h = \sqrt{1 + 42\beta^2}$, $\quad \beta = (3 - K_d)(35 - 9K_d)/192$.

In this case of $y(t)$ being the initial Gaussian signal, we do not actually have the transform yet. To develop an algorithm for the shaker controller one needs to know how to calculate an $x(t)$ instantaneous value for the given $y(t)$ value, not vice versa as in Eq. (7). Considering Eq. (7) as a cubic equation in $x(t)$, the required Gaussian-to-non-Gaussian transformation function is obtained as follows

$$x(t) = \sqrt[3]{\frac{y(t)}{2\alpha_3} + \sqrt{D}} + \sqrt[3]{\frac{y(t)}{2\alpha_3} - \sqrt{D}} \tag{9}$$

where $D = \{\alpha_1/(3\alpha_3)\}^3 + \{y(t)/(2\alpha_3)\}^2$.

It is clear that the functional transform (9) for kurtosis decrease is, in fact, not a polynomial transform as was the case for kurtosis increase. However, this post-IFFT transformation method for non-Gaussian closed-loop random testing can still be called polynomial because, in both cases of kurtosis increase and decrease, the cubic polynomial relationship (7) between the instantaneous values of the input and output signals is what the change of kurtosis value is based on.

The non-Gaussian technique of time history transformation, now for kurtosis decrease, as well as for kurtosis increase before, has an inherent tendency of introducing PSD distortions. The latter can be avoided if,

- firstly, the changes to control the kurtosis are done not after the time history is generated but in the process of this generation and,
- secondly, these changes are administered by the use of those variables that do not affect the PSD.

To develop a kurtosis control procedure satisfying these two requirements, a general equation was needed for the kurtosis being determined via the parameters involved in Eq. (1) for time history generation. This issue is addressed in the next section.

6. Kurtosis as phase-controlled parameter

The fourth PDF moment M_4 that defines the value of kurtosis can be expressed not only in terms of the PDF, as in Eq. (5), but also via $x(t)$ in the time history domain

$$M_4 = \frac{1}{T}\int_0^T \{x(t)\}^4\, dt. \tag{10}$$

A similar equation holds for a moment of any order simply by changing the power superscript in the integrand. Particularly, for the second moment it will be $\{x(t)\}^2$ instead of $\{x(t)\}^4$. The second moment M_2 is actually the RMS squared, i.e. $(M_2)^2$ can be used in Eq. (5) instead of σ^4.

For a stationary ergodic random signal, the moment M_4, or that of any other order, is found from Eq. (10) with the time history length T theoretically approaching infinity. However, for a pseudo-random signal generated according to Eq. (1), we use a finite data block whose length is $T = 1/\Delta f$. Thus, averaging of instantaneous values in a certain power in Eq. (10) is taken over period T, not infinity. Now Eq (1) can be substituted into Eq. (10), or similar equation for M_2. If the integrals obtained are taken analytically, both moments (M_2 and M_4) will be expressed in terms of the amplitudes A_n and the phase angles φ_n.

For the second moment

$$M_2 = \frac{1}{T}\int_0^T \{x(t)\}^2\, dt \tag{11}$$

$$= \frac{1}{T}\int_0^T \left\{\sum_{n=1}^{N} A_n^2 \cos^2\left(n\frac{2\pi}{T}t+\varphi_n\right) + \sum_{n_1=1}^{N-1}\sum_{n_2=n_1+1}^{N} 2A_{n_1}A_{n_2}\cos\left(n_1\frac{2\pi}{T}t+\varphi_{n_1}\right)\cos\left(n_2\frac{2\pi}{T}t+\varphi_{n_2}\right)\right\} dt$$

integration poses no problem because an integral of a product of two cosine functions from different harmonics (i.e. for different subscripts n_1 and n_2) is zero and an integral of $\cos^2(n\frac{2\pi}{T}t+\varphi_n)$ over period T is equal to 0.5. Equation (11) results in the second moment, i.e. the mean-square-value σ^2, being a function of the harmonics amplitudes only

$$M_2 = \sigma^2 = \frac{1}{2}\sum_{n=1}^{N} A_n^2 \tag{12}$$

with the phases φ_n not involved.

The latter is in line with the fact that the power spectrum does not depend on the harmonics phases. According to the definition of PSD, the area under it must be equal to the mean-square-value σ^2, i.e. the second moment M_2. Based on this, the correctness of Eq. (12) and its phase-independent character are easily verified if Eq. (2) is substituted into Eq. (12). The result

$$M_2 = \sigma^2 = \sum_{n=1}^{N} \Delta f S(n\Delta f) \tag{13}$$

is a sum of products of the height $S_n = S(n\Delta f)$ of a PSD spectrum line by its width Δf, with this product being an area of the rectangular bin corresponding to one of the PSD spectrum lines. Then, the area of all bins taken together when calculating M_2 by Eq. (13) is indeed the full area under the PSD.

It is much harder to derive an equation for the fourth moment because the fourth power in the integrand in Eq. (10) produces cosine function products with more diverse combinations of harmonics indices $n_1, n_2, \ldots$ than that in Eq. (11) which involves the second power. When all these combinations for M_4 are looked at, it appears that, after being integrated, many of them vanish similarly to how it happened to the second term of the integrand function in Eq. (11). Some of the combinations result in sum functions involving only A_n^2 as in Eq. (12) but no dependence on phases.

However, distinct from the second moment, there will be non-zero integrals resulting in additional components in M_4 that are functions of both amplitudes A_n and phases φ_n. The fourth moment equation is as follows [12,13]

$$M_4 = 3(M_2)^2 - \frac{3}{8}\sum_{n=1}^{N} A_n^4 + \frac{3}{2}\sum_{\substack{i=j+2k \\ j\neq k}} A_i A_j A_k^2 \cos(\varphi_i - \varphi_j - 2\varphi_k)$$

$$+\frac{3}{2}\sum_{\substack{i+j=2k \\ i<j}} A_i A_j A_k^2 \cos(\varphi_i + \varphi_j - 2\varphi_k) + 3\sum_{\substack{i+j=k+m \\ i<j,k<m,i<k}} A_i A_j A_k A_m \cos(\varphi_i + \varphi_j - \varphi_k - \varphi_m) \qquad (14)$$

$$+3\sum_{\substack{i+j+k=m \\ i<j<k}} A_i A_j A_k A_m \cos(\varphi_i + \varphi_j + \varphi_k - \varphi_m) + \frac{1}{2}\sum_{i=3j} A_i A_j^3 \cos(\varphi_i - 3\varphi_j)$$

When calculating kurtosis by dividing Eq. (14) by $(M_2)^2$ according to the kurtosis definition, a value of 3 emerges from the first term in Eq. (14). This is true for any pseudo-random signal (1), no matter what are its amplitudes and phases. Hence, we are looking at something originating from the Gaussian kurtosis value $K_G = 3$ but different from it because of contributions from other terms.

The second term in Eq. (14) comes with negative sign. It takes the kurtosis down from the value of 3 but this decrease is very small. For example, with 500 spectrum lines in the PSD ($N = 500$ in Eq. (1)), the kurtosis is decreased by this second term just from 3 to 2.99 approximately. For more spectrum lines the change is even smaller. The exact value of a combination of the first two terms in Eq. (14) depends on harmonics amplitudes A_n, i.e. on the PSD shape. However, no matter what the PSD is and with what harmonics phases the pseudo-random signal (1) is generated, any changes in kurtosis are so small that they do not exceed the precision of kurtosis calculation from experimental data.

Thus, with only the first two terms in Eq. (14) taken into account, the kurtosis actually remains of the Gaussian value. It is the third, fourth, fifth, sixth, and seventh terms in Eq. (14) that make the kurtosis flexible. This is due to the fact that all these terms involve not only the harmonics amplitudes A_n but the phases φ_n as well. For example, in the third term of Eq. (14), the argument of the cosine function includes the phases φ_i, φ_j, and φ_k of the same harmonic components that are present in the product of amplitudes $A_i A_j A_k^2$.

Summation in the third and subsequent terms of Eq. (14) is performed only for those combinations of subscripts i, j, k, and m that satisfy conditions written under the summation symbols. Thus, a certain relationship, such as

$$i = j + 2k, \qquad (15)$$

between the harmonics subscripts i, j, and k must be observed for this trio to form a member of the summation in the third term of Eq. (14). For hundreds or even thousands of spectrum lines in modern controllers there will be plenty of subscript groups i, j, k satisfying the condition set by Eq. (15).

If the phase angles φ_n of the harmonics are chosen in a random manner, as in the classical random testing technique discussed in the Introduction, then the cosine functions in Eq. (14) also produce random values distributed uniformly in the interval from -1 to 1. These random values corresponding to different subscript groups compensate each other and bring the result of summation close to zero as the number of the groups for all summations of this kind is large.

It means that, for random phases, not only the second term in Eq. (14), but also the third and other phase-dependent terms do not take the kurtosis away from the original value of 3. However, this can be changed if the phase selection strategy is not simply a random choice. The non-Gaussian phase selection method alters the aforementioned randomness of cosine function outputs by rearranging some of the phases from random to deterministic values in the following way.

Firstly, all phases are given random values as in the regular Gaussian simulation technique. Then, a group of three phases φ_i, φ_j, and φ_k is selected such that the three subscripts i, j, and k involved satisfy Eq. (15). The possible choices are numerous; let us take one of them $i = 100$, $j = 40$, and $k = 30$ as an example. For this group the amplitude coefficient for the corresponding member of the sum in the third term of Eq. (14) will become $A_{100} A_{40} A_{30}^2$.

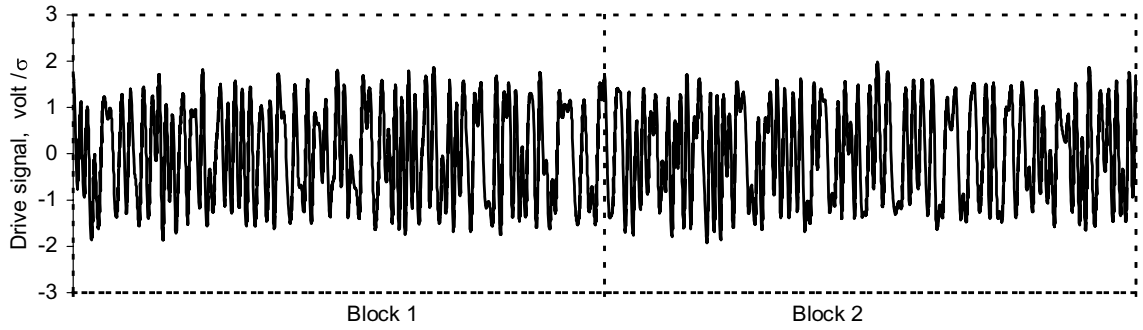

Fig. 1. Each new data block is different in the drive signal with low kurtosis.

Now, two of the phases in this group, say φ_{100} and φ_{40}, may remain random but the third phase φ_{30} is selected such that the argument of the cosine function $(\varphi_{100} - \varphi_{40} - 2\varphi_{30})$ is equal to π. With such a deterministic selection of the third phase $\varphi_{30} = (\varphi_{100} - \varphi_{40} - \pi)/2$, the cosine function will produce not a random value but the smallest possible value of -1 making this member of the summation equal to $-A_{100}A_{40}A_{30}^2$.

A similar action can be performed for the phases of other three harmonics with subscripts $l, m,$ and n also satisfying Eq. (15) such as $l = m + 2n$. By selecting φ_n calculated via two random phases φ_l and φ_m as follows $\varphi_n = (\varphi_l - \varphi_m - \pi)/2$, one more negative member $-A_l A_m A_n^2$ will be added to the aforementioned first member $-A_{100}A_{40}A_{30}^2$ of the same summation.

If the phase selection process described is continued with each next trio of harmonics not repeating those harmonics that were phase-optimized already, the result of summation in the $\sum_{i=j+2k} A_i A_j A_k^2 \cos(\varphi_i - \varphi_j - 2\varphi_k)$ term will become a negative value instead of being close to zero when all phases were random. The outcome of such a procedure, which can be also performed for other sums in Eq. (14), is that the kurtosis is decreasing from the Gaussian value $K_G = 3$.

It is clear from the above that the fact of some of the harmonic phases becoming deterministic does not imply that these phases are the same all the time while the shaker drive signal is generated. For each new data block, those phases that are supposed to be random are fixed first. Then, the remaining special phases are calculated deterministically from those phases that were prescribed randomly. It means that every subsequent data block generated according to Eq. (1) comes with a different set of harmonics phases.

Thus, the data blocks in the non-Gaussian signal with low kurtosis are all different such as in the case of the classical Gaussian pseudo-random generation technique. The non-Gaussian time history never repeats itself as can be seen in Fig. 1 that depicts two blocks of a signal with kurtosis $K = 1.7$ (each of the blocks contains 4096 data points). The labels on vertical axis correspond to 1σ, 2σ, and 3σ that is instrumental for observing the crest factor value that was $CF = 2.0$ in this example.

The phase shifts between harmonics of pseudo-random signal with non-Gaussian kurtosis will change after the signal passes through the dynamic system of a shaker and a unit under test. This will result in kurtosis moving closer to Gaussian value but it will still remain non-Gaussian. The degradation of kurtosis value can be compensated by prescribing some extra non-Gaussian kurtosis deviation when generating the drive signal. As the exact difference between the input and output kurtosis values is not known, few iterations described by Eq. (4) are still needed and, after that, the prescribed value for the output kurtosis can be achieved. All this has been accomplished in experiments and described in Reference [15].

7. Sigma clipping

The most common circumstances when sigma clipping is used have always been about getting more power from the same shaker system as discussed in Section 4. However, recently one more situation emerged when a due attention is required to clipping, or actually to a necessity of having something better than clipping to serve the

purpose of crest factor limiting. It has been reported that in the squeak and rattle testing of automobile components sigma clipping causes severe problems [8].

The basic sigma clipping procedure is straightforward: simply to cut everything that is higher than the prescribed limit and to remove it from the Gaussian drive signal. Possible clipping levels are usually expressed in controller menus as 3σ clipping, 2σ clipping or similar and this means reducing crest factor of the drive signal to $CF = 3$, $CF = 2$, etc. However, are there any unpleasant side effects associated with clipping? Furthermore, being performed on the drive signal input, how efficient is it in decreasing crest factor of the acceleration output? Both these issues will be discussed below.

If, after a drive signal is IFFT-generated, any alterations (either sigma clipping or else) are made to the time history, the drive signal spectrum will no longer correspond exactly to the given PSD. These changes in the PSD that are normally referred as harmonic distortions are spread over the entire frequency interval including both test specification bandwidth and out-of-band frequencies. For example, high frequency out-of-band distortions were pointed out as the cause of confusion in the aforementioned squeak and rattle testing [8]. When the sigma clipping was on, audible clicks similar to the sound of a rattling component were generated by the shaker itself, not by the unit under test being evaluated for squeak and rattle.

Some harmonic distortions caused by sigma clipping can be compensated in the closed-loop iterative procedure by decreasing the corresponding discrete PSD values $S^{dr}_{i+1}(n\Delta f)$ for the next iteration according to Eq. (3). But this does not work at the out-of-band frequencies or in the vicinity of sharp resonances. For the out-of-band frequencies all spectrum line amplitudes A_n are set to zero instead of Eq. (2). Hence, nothing is contributing to the time history generation by Eq. (1) and, obviously, nothing cannot be decreased further. If any PSD content is present at the out-of-band frequencies, it is caused by harmonic distortions only and will stay there as an uncontrollable noise floor in the PSD.

The harmonic distortions and the increased noise floor they produce affect not only out-of–band frequencies. The shaker armature, or test fixture, or the unit under test may have resonances where, according to Eq. (3), the controller will need very low $S^{dr}_{i+1}(n\Delta f)$ values in the drive signal PSD to match the required acceleration PSD specifications $S_{spec}(n\Delta f)$ at this spectrum line. Certainly, the controller cannot descend lower than the noise floor and, thus, the latter is the limit where the controller's ability to put the resonance further down will end.

It is clear from the above that if, as a result of sigma clipping, the PSD noise floor rises, then the controller's dynamic range (that is the difference between realizable maximum and minimum PSD values) will be reduced. This is the price to pay for sigma clipping because the wider the control dynamic range, the better the controller is in its capabilities of reproducing test specifications with big ratios between the highest peak and the lowest notch in the prescribed PSD profile.

Shaker controller manufacturers regard the dynamic range as one of the most important performance characteristics [2,19,21] and report it to be in the region of 90dB in the latest products if no clipping is used. However, a loss of available dynamic range should be expected if clipping is introduced. It would be useful to know what fraction of these 90 dB disappears for various clipping levels. Some experimental results on this matter are presented in the next section.

8. Experimental results on sigma clipping

The experiment was carried out on a Derritron VP5/DLA1050 electrodynamic shaker controlled by a PC equipped with a National Instruments PCI-MIO-16E-4 DAQ board and LabView 7.0 software to accomplish digital-to-analog and analog-to-digital conversion of the signals. Kurtosis and crest factor were evaluated using data samples of 80 blocks of 4096 data points each. The power spectrum was analysed with 2000 spectrum lines and the frequency increment $\Delta f = 2$ Hz. The target PSD profile was a uniform spectrum from 20 to 180 Hz and zero everywhere else.

Figure 2a depicts a Gaussian drive signal with no clipping. It has the crest factor of $CF = 4.4$. As can be seen in Fig. 2b, the specified PSD profile was realized experimentally with the drive signal dynamic range DR = 80 dB. This drive input has produced an acceleration output signal (Fig. 2c) also with $CF = 4.4$. The acceleration PSD obtained is shown in Fig. 2d and the dynamic range in it appears to be DR = 33 dB. This value is less than in commercial controllers but still enough to see the tendencies discussed below.

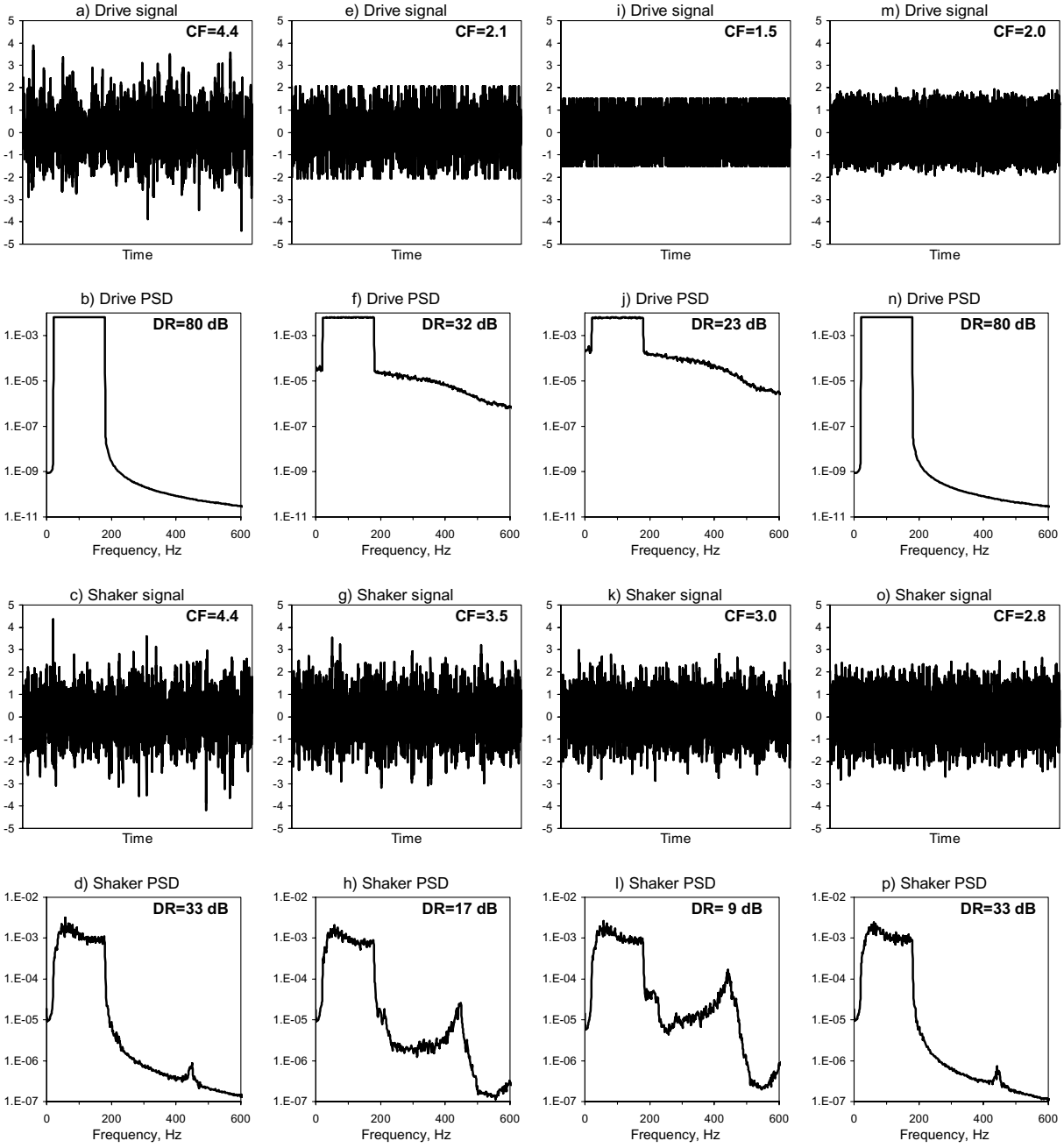

Fig. 2. Experimental results for no clipping (a,b,c,d), 2σ clipping (e,f,g,h), 1.2σ clipping (i,j,k,l), and non-Gaussian phase selection method (m,n,o,p).

With clipping added the crest factor values are expected to change. First, the 3σ clipping (that is a popular test specification) was tried but no noticeable change was observed in the acceleration output crest factor compared to the above value with no clipping. This is not a surprise for those who have ever checked the actual crest factor of the shaker table acceleration after setting up a certain clipping level for the drive signal. They know that the shaker system partially restores peak heights. This phenomenon has been also reported by shaker equipment manufacturers [7].

Harder clipping, down to 2σ level (Fig. 2e), was required in our experiment to reduce the acceleration crest factor

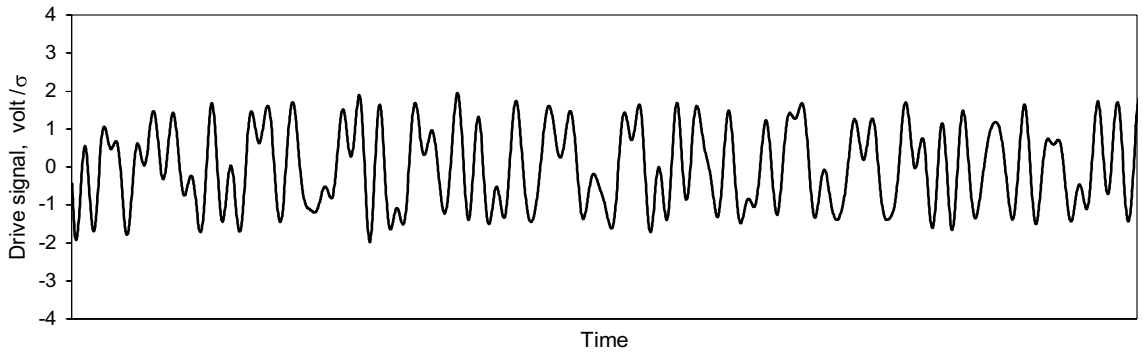

Fig. 3. Fragment of the non-Gaussian drive signal with kurtosis K=1.7 and crest factor $CF = 2.0$.

from 4.4 to 3.5 (see Fig. 2g). However, there was a price to pay for this moderate decrease in crest factor. At the out-of-band frequencies the acceleration PSD (Fig. 2h) had a much higher level then that with no clipping (Fig. 2d). Half of the control dynamic range has been lost. This is the result of the drive signal dynamic range in Fig. 2f being only 32 dB instead of DR = 80 dB for no clipping in Fig. 2b.

Clipping as low as 1.2σ (Fig. 2i) was required to achieve the real 3σ specification, i.e. to contain the acceleration output, not input, within $\pm$ 3σ limits (Fig. 2k). However, in this case, almost nothing (just 9 dB) remains as an available acceleration dynamic range (see Fig. 2l) with the drive signal dynamic range decreased from 80 to 23 dB (Fig. 2j) by this severe clipping. The drive signal clipped at 1.2σ actually had crest factor $CF = 1.5$ because the signal RMS was reduced after all time history points higher than the clipping level were removed.

There is a limit to the acceleration crest factor decrease that can be accomplished by clipping. In our experiment, the result shown in Fig. 2k was the best that could be obtained with clipping. Further clipping beyond 1.2σ gave no improvement. The acceleration crest factor never went down and stayed around 3σ. The reason for this predicament is that the harmonic distortions from severe clipping are so strong that the noise generated by them becomes comparable with the useful control signal. When the noise component with probability distribution close to Gaussian is increasing, its higher peaks dominate the opposite tendency in the clipped main component. That is what prevents the crest factor of the output acceleration signal from following the controller's command for further peak limiting.

9. Kurtosis decrease versus sigma clipping

As discussed in Section 6, the phase angles φ_n in the IFFT procedure can be manipulated so that the kurtosis value of the signal generated by Eq. (1) becomes lower. The amplitudes A_n remain responsible for the PSD as in the common Gaussian technique. That is what the special phase selection method for non-Gaussian random shaker testing is about. The results obtained by this method for the same experimental setup described in the previous section are as follows.

A non-Gaussian drive signal with kurtosis $K = 1.7$ is shown in Fig. 2m and its magnified fragment is depicted in Fig. 3. The signal was generated for the same target PSD profile as that used in the Gaussian experiment (Fig. 2a, b, c, d). Now, with the non-Gaussian random simulation (Fig. 2m), the crest factor is $CF = 2.0$, down from the value of $CF = 4.4$ for the Gaussian drive signal in Fig. 2a. Despite of such a drastic modification of the time history, the PSD of non-Gaussian signal (Fig. 2n) has exactly the same low tail for out-of-band frequencies as that of the PSD of the Gaussian drive signal (Fig. 2b).

The PSD noise floor for the non-Gaussian simulation by phase selection (Fig. 2n) remains where it was for the traditional Gaussian simulation in Fig. 2b. It means that the drive signal dynamic range is maintained (in this experiment at DR = 80dB). After the drive signal sigma limiting was achieved without compromising the out-of-band frequencies, the dynamic range of the shaker acceleration signal is expected to be as good as for the basic Gaussian simulation and this is confirmed by comparison of Fig. 2d and 2p.

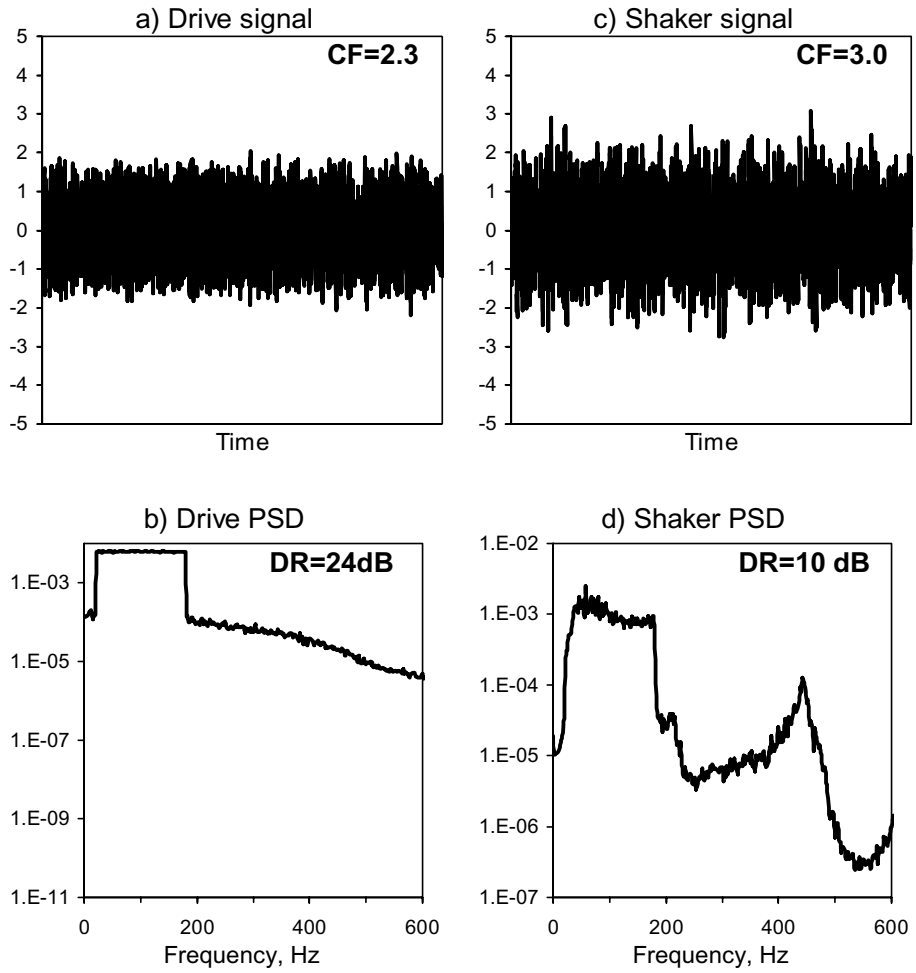

Fig. 4. Experimental results for non-Gaussian polynomial transform method.

As for the non-Gaussian acceleration time history (Fig. 2o), its kurtosis appears to be $K = 2.3$ with the crest factor $CF = 2.8$. The latter is much better than $CF = 3.5$ obtained with clipping at the same 2σ level (Fig. 2g) and even lower than the best clipping result ($CF = 3.0$) observed in the experiment with 1.2σ clipping (Fig. 2k). The difference between $CF = 3.0$ and $CF = 2.8$ might look nonessential but the former comes with the input and output dynamic ranges of 23 and 9 dB whereas the latter has impressive 80 and 33 dB, which are exactly the same as in the Gaussian mode of controller operation.

The polynomial transform has been also tried experimentally. It was set up to decrease kurtosis of the drive signal to the same value of $K = 1.7$ as by the phase selection method. The crest factor decrease for the drive signal (Fig. 4a) was close to that with the phase selection (Fig. 2m) but the harmonic distortions and the subsequent loss of dynamic range were as bad as with clipping, both for the drive signal (Fig. 4b) and the shaker acceleration (Fig. 4d).

10. Conclusions

Reducing the crest factor of a random shaker excitation by sigma clipping is a well-known practice but it brings about frequency distortions which upset the shaker controller operation. The kurtosis decrease by polynomial transform method is also an enforced alteration of the Gaussian pseudo-random drive signal, maybe less radical than clipping but still changing the time history.

Such changes, either from clipping or polynomial transformation, result in substantial losses of the controller's dynamic range. This outcome is unavoidable as long as changes are made to the drive signal after it has been IFFT-generated, no matter if these changes are truncation by clipping, or polynomial re-shaping the peaks, or anything else. The phase selection method is different since it decreases kurtosis and crest factor not after but in the process of the IFFT signal generation.

When phase selection is used for non-Gaussian shaker simulation, the multi-frequency character of the pseudo-random signal remains intact with absolutely no alterations from the combination of pure sinusoidal components. Thus, there are no harmonic distortions passed to other frequencies as it is the case for clipping or polynomial transform. With the phase selection method, one can manage to preserve the PSD dynamic range while being able to decrease kurtosis such that the crest factor is substantially reduced. It means that more powerful excitation can be obtained from the same shaker system because an extra space is created between the peaks of reduced height and the system abort limit.

If the power restriction comes from the amplifier capabilities then it matters what has been achieved with the drive signal crest factor. The fact that it was reduced from 4.4 to 2.0 allows to increase the drive signal RMS twice and still stay comfortably within the amplifier input peak limits. This new drive signal will be 4 times more powerful than before. In the case of the shaker armature overstroke being the power restriction, the acceleration feedback crest factor decrease from 4.4 to 2.8 means that the shaker power can be doubled in tests where the PSD is the only test specification prescribed.

References

[1] R.J. Allemang and D.L. Brown, Experimental modal analysis, in: *Harris' Shock and Vibration Handbook*, C.M. Harris and A.G. Piersol, eds, Ch 21, McGraw Hill, 2002, pp. 21.1–21.72.

[2] Control system dynamic range, *Spectral Dynamics Technical Note*, http://www.spectraldynamics.com/dynamic_range.htm.

[3] D.J. Ewins, *Modal Testing: Theory, Practice and Applications*, Research Studies Press Ltd, 2000.

[4] A. Kawata and Y. Yamauchi, Non-Gaussian random vibration testing beyond the conventional testing – On the progress of mathematical method, *Journal of Packaging Science & Technology* **15**(5) (2006), 237–243.

[5] N.M.M. Maia and J.M.M. Silva, *Theoretical and Experimental Modal Analysis*, Research Studies Press Ltd, 1997.

[6] Non-Gaussian random control, *Unholtz-Dickie News*, http://udco.com/news.shtml#Gaussian.

[7] P. Rogers, Aggressive low frequency random vibration, *Sound and Vibrations* **39**(10) (2005), 8–9.

[8] M.A. Schneider and E.L. Peterson, Developing robust vibration excitation and control methods for evaluating rattle noise in automotive components, *SAE paper1999-01-1725, Proceedings of the Noise and Vibration Conference*, Traverse City, MI, 1999, 1–7.

[9] E.A. Sloane and C.L. Heizman, Vibration control system, *US Patent 3,848,115*, 12 November 1974.

[10] D.O. Smallwood, Generating non-Gaussian vibration for testing purposes, *Sound and Vibrations* **39**(10) (2005), 18–24.

[11] D.O. Smallwood, Generation of stationary non-Gaussian time histories with a specified cross-spectral density, *Shock and Vibration* **4**(5/6) (1997), 361–377.

[12] A. Steinwolf, *Analysis and Simulation of Non-Gaussian Random Vibrations*, Naukova Dumka, Kiev, 1993 (in Russian).

[13] A. Steinwolf, Approximation and simulation of probability distributions with a variable kurtosis value, *Computational Statistics and Data Analysis* **21**(2) (1996), 163–180.

[14] A. Steinwolf, Closed-loop shaker simulation of non-Gaussian random vibrations; Part 1 Discussion and methods, *Test Engineering and Management* **68**(3) (2006), 10–13; Part 2 Numerical and experimental results, *Test Engineering and Management* **68**(5) (2006), 14–19.

[15] A. Steinwolf, Random vibration testing beyond PSD limitations, *Sound and Vibration* **40**(9) (2006), 12–21.

[16] A. Steinwolf, Shaker simulation of random vibrations with a high kurtosis value, *Journal of the Institute of Environmental Sciences* **XL**(3) (1997), 33–43.

[17] A. Steinwolf, True-random mode simulation of non-Gaussian vibrations with high kurtosis value, *Proceedings of the 46th IEST Annual Technical Meeting*, Providence, RI, 2000, 148–155.

[18] K. Ueno and K. Imoto, Vibration control system, *US Patent 5,012,428*, 30 April 1991.

[19] P. Van Baren and G.F. Lang, Examining the dynamic range of your vibration controller, *Sound and Vibration* **41**(8) (2007), 12–20.

[20] J. Van Baren and P. Van Baren, The third dimension of random vibration control, *SAE Paper 2007-01-2270, Noise and Vibration Conference and Exhibition*, St Charles, IL, 2007, 1–10.

[21] Vibration test systems, *LDS Knowledge Base*, http://www.lds-group.com/docs/knowledge_base.php?application_id=2.

[22] S.R. Winterstein, L. Manuel and O.B. Ness, Nonlinear dynamic responses of marine structures under random wave loads, *Proceedings of the 5th Int. Conference on Structural Safety and Reliability*, San Francisco, 1989, 159–166.